Journal of Manufacturing Processes 48 (2019) 199–209

Contents lists available at ScienceDirect

Journal of Manufacturing Processes

journal homepage: www.elsevier.com/locate/manpro

Investigation the effect of pulsed laser parameters on the temperature distribution and joint interface properties in dissimilar laser joining of austenitic stainless steel 304 and Acrylonitrile Butadiene Styrene

Yeping Peng[a], Azeez A. Barzinjy[b,c], Abdullah A.A.A. Al-Rashed[d], Afshin Panjehpour[e], Mehdi Mehrjou[e], Masoud Afrand[f,g,*]

[a] Shenzhen Key Laboratory of Electromagnetic Control, College of Mechatronics and Control Engineering, Shenzhen University, Shenzhen, 518060, China
[b] Department of Physics, College of Education, Salahaddin University-Erbil, Kurdistan Region, Iraq
[c] Department of Physics Education, Faculty of Education, Tishk International University, Erbil, Kurdistan Region, Iraq
[d] Department of Automotive and Marine Engineering Technology, College of Technological Studies, The Public Authority for Applied Education and Training, Kuwait
[e] Department of Mechanical Engineering, Najafabad Branch, Islamic Azad University, Najafabad, Iran
[f] Laboratory of Magnetism and Magnetic Materials, Advanced Institute of Materials Science, Ton Duc Thang University, Ho Chi Minh City, Vietnam
[g] Faculty of Applied Sciences, Ton Duc Thang University, Ho Chi Minh City, Vietnam

ARTICLE INFO

Keywords:
Laser joining
Dissimilar materials
Acrylonitrile Butadiene Styrene
Adhesive zone

ABSTRACT

Direct laser joining of metal to plastic materials is one of the cost effective methods of joining. The demand for laser welding of stainless steels and thermoplastics is going on increase because of having many applications such as automotive, aerospace and aviation industries. This paper presents the experimental investigation of direct laser joining of stainless steel 304 and Acrylonitrile Butadiene Styrene (ABS). The effects of pulsed laser parameters including laser welding speed, focal length, frequency and power on the themperature field and tensile shear load was investigated. The results showed that excessive increase of the joint interface temperature mainly induced by high laser power density results in exiting of the more volume of the molten ABS from the stainless steel melt pool. Also, increasing the laser power density through decreasing the focal length or increasing the laser power led to an increase in the surface temperature, higher beam penetration and high volume of molten ABS. Decreasing the focal length from 5 to 2 mm significantly rose the temperature from 150 to 300 °C. By increasing the laser pulse frequency, the number of bobbles at the ABS interface surface remarkably increased where the temperature increased from 120 to 180 °C. The X-ray spectroscopy results showed the existence of the polymer elements on the metal surface at the joint interface zone. The tensile shear load clearly increased from 280 to 460 N with augmentation of laser average power from 180 W to 215 W. Applying higher levels of laser power has clearly decreased the tensile shear load due to creating bigger bobbles and more cavities at the adhesive zone.

1. Introduction

Contemporary products are not conceivable without interconnection between different materials, whether between different metals or even metals-polymers and composites [1–4]. Laser joining of metal and plastics has emerged as a promissing technique that has many advantages over the conventional methods of joining such as adhesive bonding [5–7]. Dissimilar welding of metal and plastic materials has composed of bonding or fusion zone which in turn can produce a bonding zone or metals-polymer interconnection from very thin sheets thickness about 0.01 mm to 50 mm. Nowadays, the demand for direct laser joining of metal-polymer materials has considerably increased for many applications in different industries such as automotive, medical, electronics, etc. Laser joining can remarkably increase efficiency of hybrid metal-polymer joints to reduce the time of production and the weight of the structures [8,9]. Laser welding of dissimilar materials with the presence of protective gas such as helium, argon and nitrogen, produces high quality joint with good performance, high speed, high flexibility and low distortion. Numerous studies have been done to investigate the laser welding of dissimilar materials either metals or

Abbreviation: ABS, Acrylonitrile Butadiene Styrene; HAZ, Heat Affected Zone

* Corresponding author at: Ton Duc Thang University, Ho Chi Minh City, Vietnam.
E-mail addresses: azeez.azeez@su.edu.krd (A.A. Barzinjy), masoud.afrand@tdtu.edu.vn (M. Afrand).

https://doi.org/10.1016/j.jmapro.2019.10.021
Received 14 September 2019; Received in revised form 9 October 2019; Accepted 14 October 2019

Nomenclature

D_p	Pulse duration (ms)
f	Frequency (Hz)
F_l	Focal Length (mm)
I	Current (A)
P	Power (W)
T	Temperature (K)
t	Time (s)
V	Weldingspeed (mm. s^{-1})

polymers. Ai et al. [10] studied the laser welding of polyethylene terephthalate (PET) and titanium alloys. They evaluated the geometric dimensions using a fiber laser. A transient numerical model has developed so as to predict the molten pool geometry and fluid flow of the melt pool and the possibility of porosity formation. Moreover, the temperature field and molten flow have been evaluated by changing the laser power and welding speed. The results demonstrated the frequent formation of porosity in high temperature regions and the molten pool was formed with a circular vortex flow pattern only in the PET. It was shown that the welding process parameters have important effects on the fluid flow thereby the heat transfer rate.Wang et al. [11] estimated the dissimilar laser welding of titanium and polyethylene terephthalate (PET). The results showed that welding speed plays a key role in order to achieve higher strength of the joint. Noha et al. [12] have performed optimization of the laser joint between stainless steel 304 and ABS polymer using the continuous wave fiber (CW) lasers. It was shown that a concentrated beam with power of 230 W and welding speed of 16 mm/s was known as optimal laser welding condition to obtain better and more reliable welding. Furthermore, the welding speed and laser power had the greatest effect on the weld strength. Cenigaonaindia et al. [13] studied the laser welding of polyamide and stainless steel 304. In this study, the optimal process parameters such as process speed, joint path and laser power were used to strengthen the bond structure by increasing the amount of polymer seals in the metal surface cavities. It was reported that adequate heat flow is of the essence to achieve a reliable joint. In other words, the low temperature during the process produces the low quality joint whereas the high temperature can weaken the polymer. Pelsmaeker et al. [14] studied the joining of different thermoplastic polymers through the laser welding. It was reported that joining of transparent polymer layers has got feasible at different wavelength range, which improves the sealing of micro fluidic devices. According to the mechanical tests, some of the thermoplastic polymers showed sufficiently strong bonding to allow the creation of leak-proof micro fluidic devices by using the laser welding at a specific wavelength.

Generally excessive laser heating may cause thermal damage at the polymer or plastic side of dissimilar weld during laser joining process, which deteriorates the mechanical properties of the metal-plactic joint [15]. The porosity or bobble formation at the plastic-metal interface of the laser joint may increases the possibility of the stress concentration and thereby reduces the effective mechanical strength. As a result, the joint may fail at the region of porosity concentration. Therefore, investigation the mechanism of porosity formation and effective control of porosity formation has been investigated in different studies. Zhang et al. [16] studied reduction of porosity formation in laser-joining of carbon fiber reinforced polymer and steel through appling surface modification method. They reported that by adopting this technique, the porosity could be reduced from 7.13% to 1.26%. The temperatue induced by laser heating at the joint interface has an important role on creating porosities adjacent of the bonding interface because of high temperature gradient of this region. [15,17]. Hussein et al. [18] conducted an experimental study of dissimilar laser welding of PMMA and stainless steel 304 by using ND: YAG pulsed laser. Due to the

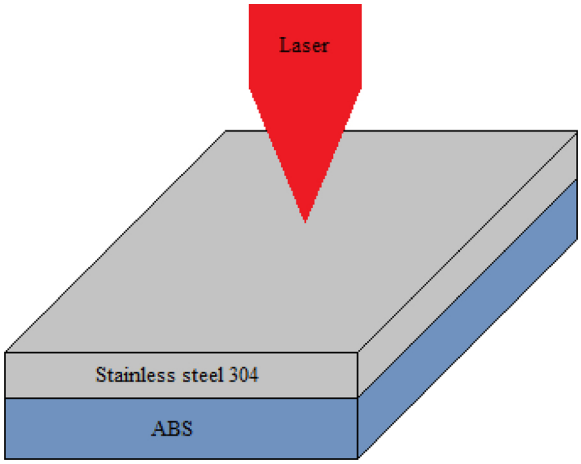

Fig. 1. Sketch of the welding configuration.

transparency of polymer, both the stainless steel and polymer can be irradiated when the welding is done. They reported that excessive increase in the laser power density has caused the augmentation of bubble formation in the polymer. Bhattacharya et al. [19] investigated the dissimilar laser welding of Polycarbonate and acrylic. They also evaluated the effects of welding process parameters including the laser power, speed and frequency on HAZ and molten pool geometry using an experimental study. It was concluded that the power and speed have an important influence on the melt pool width. Also, increasing the speed decreased the melt pool and HAZ width. Lambiase et al. [20] conducted a research on laser-assisted metal to polymer direct joining to validate finite element model. They concluded that the quality of the joints is strongly affected by the temperature field produced during the laser treatment because of the adhesion of the plastic to the metal sheet and development of bubbles (on the plastic surface) which highly depends on the temperature that polymer reached at the joint interface. The suitable temperature ought to be higher than the softening temperature, but lower than the degradation temperature of the polymer. So, the temperature distribution is of a high importance for doing this process. The Polycarbonate sheet and AISI 304 stainless steel were treated by means of high power diode laser and the effects of the process parameters (i.e. laser power and scanning speed) on the temperature were analyzed. Comparison of the experimental measurements and the finite element model for prediction the thermal field shows that there is a good agreement between the developed model results and the experiments data.

Laser assisted joining of dissimilar metal-polymer including Al-Mg alloy and Polyetheretherketone has been experimentaly performed to investigated the effect of the diode laser welding process parameters on the mechanical properties of the joints. It was reported that the average joint strength met the value of 30 Mpa at the optimum welding condition [21]. Dissimilar laser joining of transparent Polyethylene

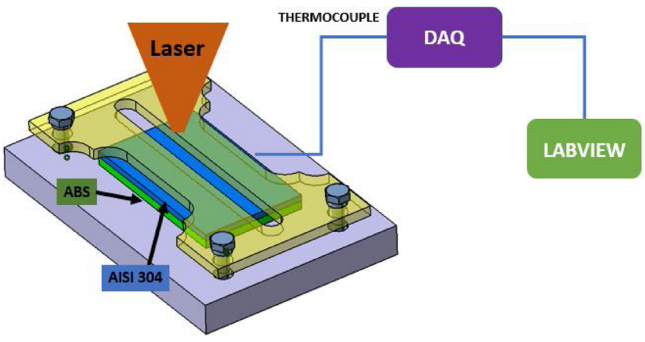

Fig. 2. Schematic diagram of the welding configuration.

Table 1
Laser welding parameters.

Test number	Pulse duration D_p (ms)	Frequency f (Hz)	Welding speed V(mm/s)	Current I (A)	Focal length F_l (mm)	Power (W)
1	8	15	4.2	130	5	215
2	8	15	4.2	130	2	215
3	8	15	6.2	130	5	215
4	10	10	6.2	130	5	192
5	10	15	6.2	130	5	250
6	8	15	8.2	130	5	215
7	8	20	6.2	130	5	225
8	6	15	6.2	130	5	178
9	10	20	6.2	100	5	209
10	8	15	6.2	150	5	256
11	8	15	6.2	150	1	256
12	8	15	6.2	150	4	256
13	8	15	6.2	100	5	185

Table 2
Welding parameters in tests 1, 3, 6.

Test number	Pulse duration (ms)	Frequency (Hz)	Current (A)	Focal length (mm)	Power (W)	Welding speed (mm/s)
1	8	15	130	5	215	4.2
3	8	15	130	5	215	6.2
6	8	15	130	5	215	8.2

terephthalate to aluminum 7075 sheets has been studied by a diode laser. The effeects of the laser power and scan speed were investigated on the quality of the joint and the process parameters were optimized using response methodology [22]. Chen et al. [23] studied the laser transmission welding of fiberglass-doped polypropylene and ABS through the experimental and numerical methods. Due to low laser transmition of ABS, this material is welded more difficult than other pure plastics. They proposed a relationship between the welding parameters, molten pool area and shear strength in the welding fiberglass-doped PP and fiberglass-doped ABS. New hybrid heat source model was developed to make three-dimensional finite element model for predicting the temperature distribution and molten pool geometry. Furthermore, a group of taguchi experiment was selected to assess the accuracy of hybrid heat source model under various welding parameters to obtain the characteristics of welded joint.

Application of joining dissimilar materials such as stainless steel 304 and ABS has remarkably increased in different industries. Seemingly, dissimilar direct laser joining of metal-polymer materials is one of the most practical methods that could be taken into account because of having much potential. Hence, experimental study of laser joining of stainless steel 304 and ABS has been carried out in order to investigate the effects of different process parameters on temperature field produced during the laser treatment which in turn directly influences the phenomena of the adhesion the plastic to the metal sheet and controlling the amount of bubbles formed in ABS at the joint interface. Analyzing the temperature variation during the laser joining process can adequately control the effects of the process parameters on the quality of the joint either mechanical properties or surface appearance of the joint for industrial applications. Additionally, variation of tensile shear load related to size of the adhesive region for the stainless steel and ABS interface in welding zone have been investigated.

2. Experiments

Austenitic stainless steel 304 with 1 mm thickness was selected with dimensions of 50 mm length and 40 mm width. Also, ABS sheet with 2 mm thickness and dimensions of 50 mm length and 40 mm width was considered. For measuring the temperature by thermocouples, two grooves created at the depth of 1 mm for thermocouple placement on the surface of stainless steel sheet. The best arrangement for welding of these two materials was placing the metal above the ABS sheet (see Fig. 1).

According to this placement, not only the welding process will be more feasible but also measurement of the temperature will be performed easier. For welding experiments, pulsed Nd:YAG laser model IQL-10 was used. The maximum average power of the machine is 500 W, the wavelength is 1.06 μm and the output frequency range is 1–250 Hz. Argon gas with pressure of 3 bars was utilized as means of protective gas. A schematic diagram of the welding configuration is shown in Fig. 2. One K type thermocouple with 1 mm diameter has been used to measure the temperature, with an operating temperature range of −40 °C and +1260 °C and the accuracy between ± 1%. The thermocouple data was recorded using the data acquisition card (model: Advantech USB 4718). The steel is mounted on the ABS plate by through the fixture with four bolts and 60 N × cm torque for each bolt to make a tight contact between plates.

Investigation of the molten pool microstructure and dimension were

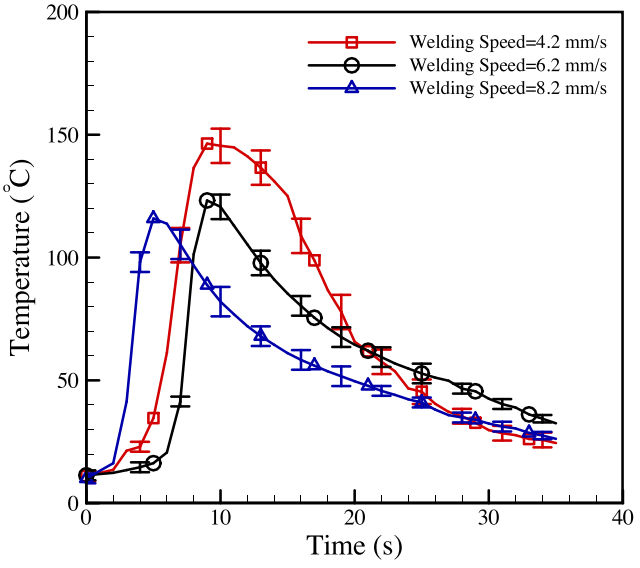

Fig. 3. Experimental results of temperature distribution versus time as a function of welding speed.

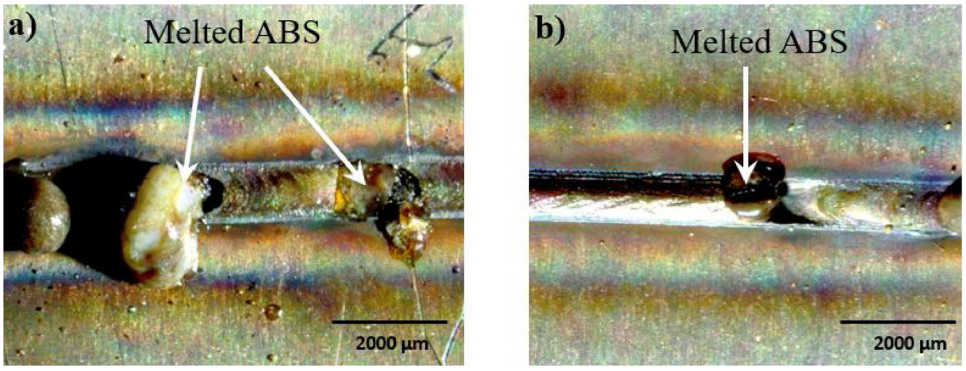

Fig. 4. Weld bead appearance on the stainless steel surface at welding speed.of a) 4.2 mm/s, b) 8.2 mm/s.

Table 3
Welding parameters in tests 1, 2.

Test number	Pulse duration (ms)	Frequency (Hz)	Current (A)	Focal length (mm)	Power (W)	Welding speed (mm/s)
1	8	15	130	5	215	4.2
2	8	15	130	2	215	4.2

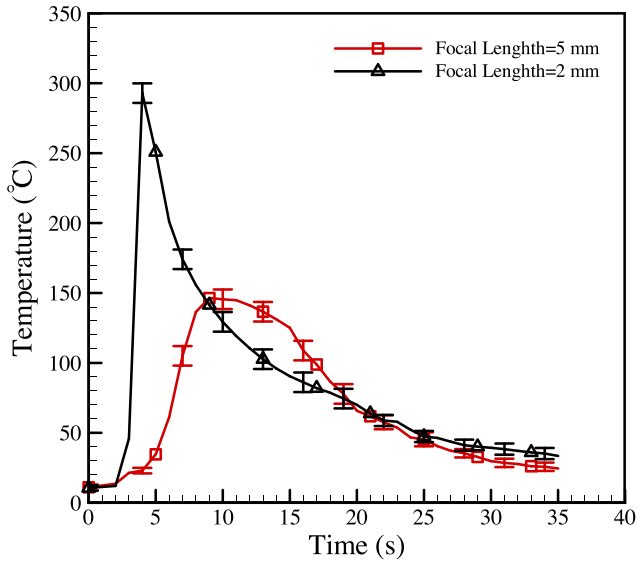

Fig. 5. Experimental results of temperature distribution versus time as a function of focal length.

performed by standard metallography methods. All the samples were mounted, polished using the standard metallographic techniques (100, 200, 400, 600, 800, 1200, 2000, and 2500 grit) and etched using Glysrzhya reagent. Finally, the SZ-X16 OLYMPUS stereoscope was used to measure the molten pool dimensions. Materials phase identification and qualification was conducted by X-ray diffraction with GNR X-ray explorer and data analysis was done using SAX program.

3. Results and discussion

In the following, the effect of process parameters on the temperature distribution and melt pool area is presented based on the experimental tests results. Pulsed laser parameter are frequency, average power, focal length and pulse duration. Welding speed is selected as means of other variable. Table 1 shows the different process parameters and their levels used in the experiments.

3.1. The effect of process parameters on the temperature distribution

3.1.1. Effect of welding speed

As shown in Table 2, in the first series of the experiments (1, 3, 6 test No) the welding speed was changed while parameters remained constant.

By comparing the results, it can be noted that with increasing the welding speed, the measured temperature values by thermocouples decreased. As shown in Fig. 3, increasing the welding speed from 4.2 to 8.2 mm/s, clearly reduced the temperature around the molten pool from 147 °C to 115 °C. Generaly, increasing the speed decreases the time of interaction between the laser beam and the workpiece and the total amount of input energy from laser beam to the substance evidently diminishes per time unit. Moreover, the temperature of the joint at the metal-plastic interface clearly changes by speed. In other words, at the higher welding speed, the lower temperature is observed and thereby the maximum temperature is lower. So the volume of the melted ABS or bursting of ABS bobbles and cavitation of stainless steel molten pool remarkably decreased during the welding process when the welding speed increased from 4.2 to 8.2 mm/s. (see Fig. 4).

3.1.2. Effect of focal length

In the second series of experiments (No. 1, 2) the decrease in focal length is observed in Table 3 while other parameter remained unchanged. Generally, reducing the beam spot size via decresing the nozzle gap from the workpiece surface results in increasing total laser beam energy density. Not only it is expected that the surface temperature grows remarkably but also the beam penetration in the substances is increased.

As shown in Fig. 5, the surface temperature of the metal in experiment No. 2 significantly increased (from 150 °C to 290 °C). Increasing power density has direcly impact on augmentation of the beam absorbtion. So, the beam is penetrated more into the molten pool or even ABS subsurface layers. Investigation the images of the bonding surface between metal and plastic (Fig. 6) reveals the fact that some metal particles is seen on the plastic surface, as well as some plastic on the metal surface, indicating a combination of metal and plastic in the contact area of the two materials. In experiment No. 2 (Fig. 6), it was observed that the laser energy has completely penetrated in the metal and the molten region and even polymer surface. Cavities on the surface of the metal and the polymer reveals this fact. Formation of the cavities, bonding and adhesion of the particles of plastic and metal implies the

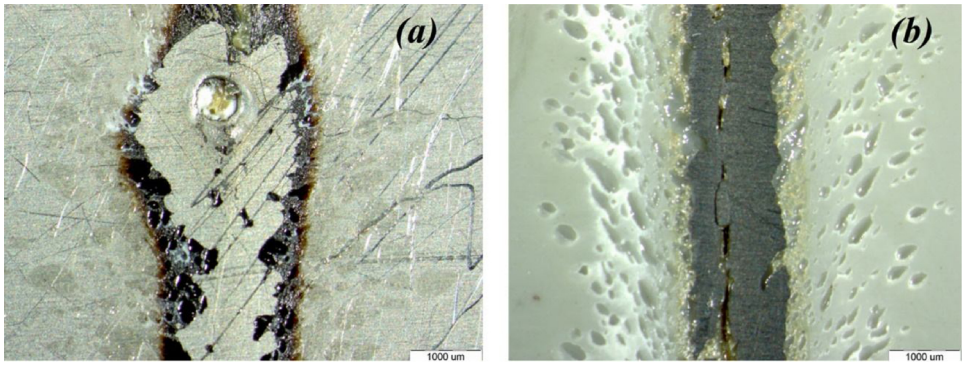

Fig. 6. The detached surface apperance after welding in test 2: (a) stainless steel 304, (b) ABS.

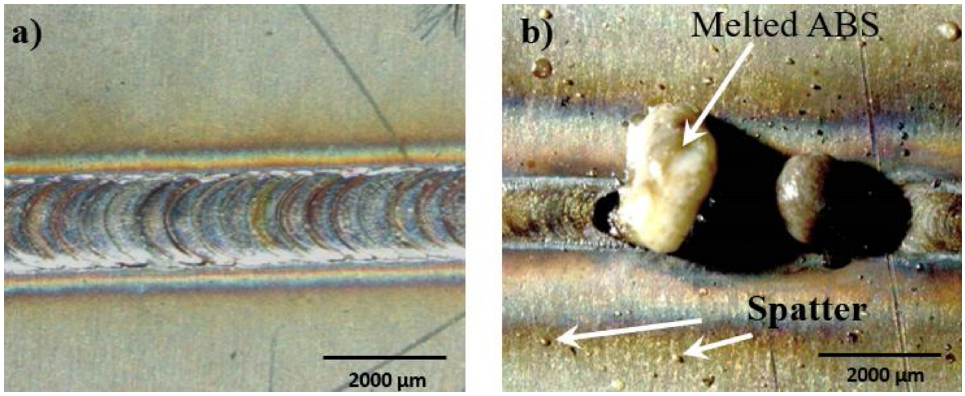

Fig. 7. Weld bead appearance of steel surface at different focal lengths of a) 5 mm, b) 2 mm.

Table 4
Welding parameters in tests 4, 5.

Test number	Pulse duration (ms)	Frequency (Hz)	Current (A)	Focal length (mm)	Power (W)	Welding speed (mm/s)
4	10	10	130	5	192	6.2
5	10	15	130	5	250	6.2

effects of laser penetration on the surface of the both metal and plastic at the interface zone. By going outward from the center of the laser beam, the temperature was reduced and only the effect of melting and heating of the plastic lower amount of bobbles were detected.

In Fig. 7, the appearance of a weld bead on the stainless steel is seen. Due to decreasing focal length more fumes and plasma plume and spatters were produced during welding at higher power density. By decreasing the focal length, not only the bead width was reduced but also more melted ABS is seen at the center of the radiation field. Hence, it could be said that the beam has penetrated more deeper than interface surface and meted ABS has exited from the steel molten pool (see Fig. 7).

3.1.3. Effect of pulse frequency

The third series of experiments was performed to investigate the effect of frequency on the temperature Welding parameters are observed in Table 4. Increasing the pulse frequency led to the increase of pulse repetition rate and thereby the rise in average power while other parameters such as pulse duration, current and focal length were kept unchanged.

Comparing the tests No. 4 and 5, shows that increasing the frequency from 10 Hz to 15 Hz has increased the amount of laser emmited energy per unit time and also the measured temperature by the thermocouples (see Fig. 8). On the other hand, by increasing the pulse

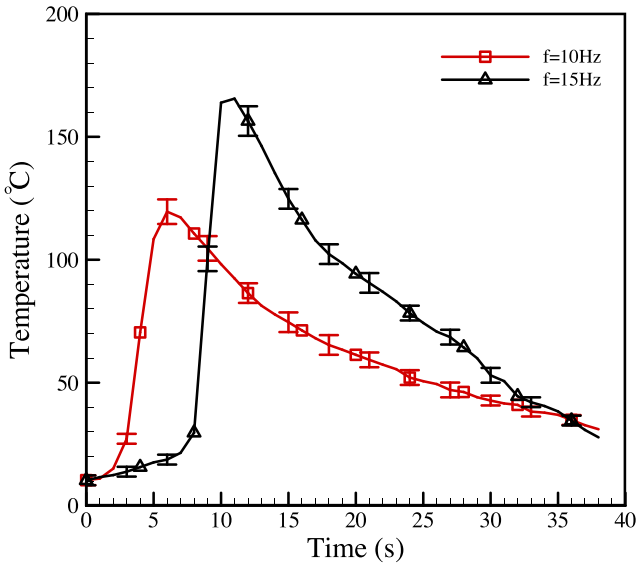

Fig. 8. Experimental results of temperature distribution versus time as a function of laser frequency.

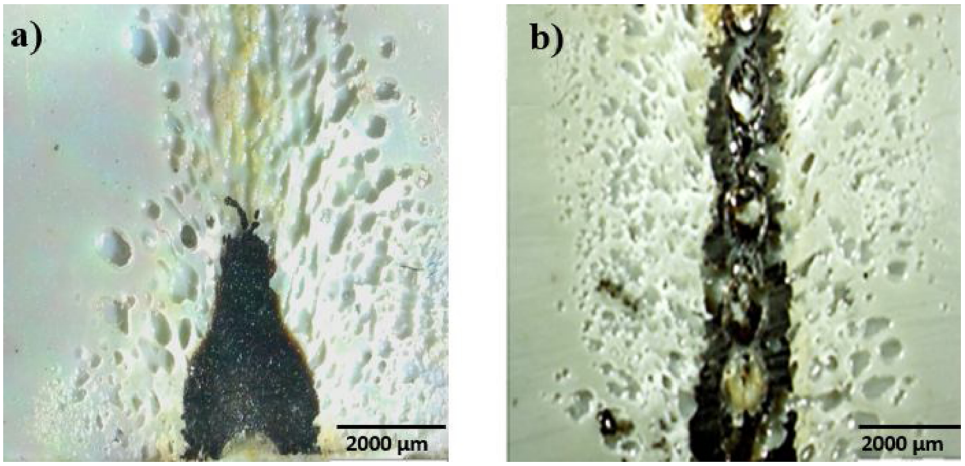

Fig. 9. Interface surface of the ABS after welding at different pulse frequency for (a) 10 Hz, (b) 15 Hz.

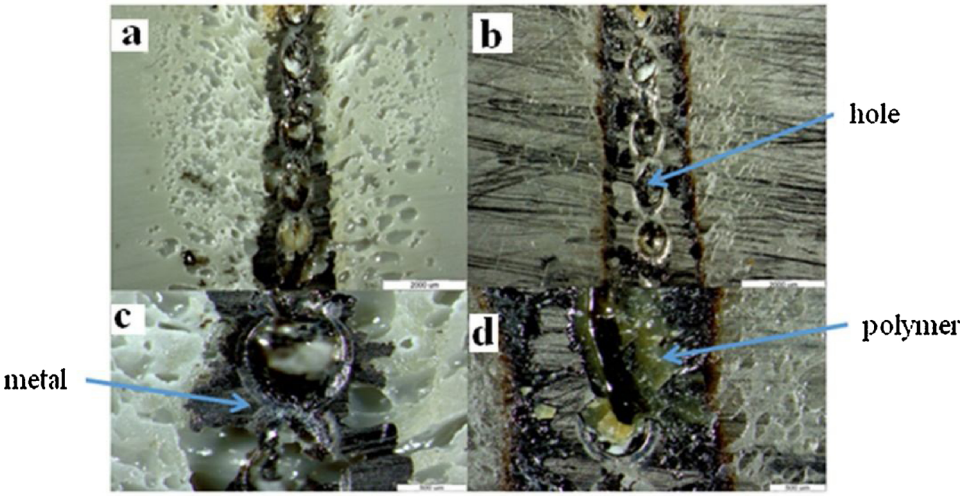

Fig. 10. Surfaces of metal and polymer after welding with different magnifications in the experiment 5: (a), (c) polymer ABS, (b), (d) stainless steel 304.

Table 5
Welding parameters in tests 3, 10.

Test number	Pulse duration (ms)	Frequency (Hz)	Current (A)	Focal length (mm)	Average Power (W)	Welding speed (mm/s)
3	8	15	130	5	215	6.2
10	8	15	130	5	256	6.2

frequency and the average power not only the penetration depth of the laser beam at the interconction surfaces of ABS and the metal was increased, but also the number of bobbles significantly increased as shown in Fig. 9.

The main reason of this phenomenon could be higher number of heating and cooling cycles induced by laser beam that results in higher amount of bobbles and cavities at the ABS surface. Moreover, Cavities on the metal surface represent the penetration of the laser beam inside the molten pool in the metal and even the melting area of the plastic. Therefore, there is a metal-plastic compound melting zone in the metal-plastic bonding region. The plasma pulme fromed at the joint interface due to interaction of laser beam with both the steel and polymer created the holes at the fusion zone which vaporized the ABS surface (see Fig10).

Thanks to diffusion of plastic and metal inside each other, a strong bond was formed although the number of bobbles has increased clearly. Fig. 10 depicts the cavities formed on the surface of the polymer. Also, the particles of the polymer on the surface of the metal and the particles of the metal on the polymer surface seen.

3.1.4. *Effect of laser beam power*

Usually, increasing the current leads to the rising the laser beam power. By increasing the current from 130 to 150 amps (according to the Table 5), the laser average power was increased from 215 to 256 W. Commonly, augmentation of laser average power has a direct influence on the penetration depth in laser welding and the amount of the heat input to the work piece. evidently, The most important effect of increasing average power is increasing the pulse energy. In Fig. 11, the comparison of the stainless steel temperature near the melt pool in experiments No. 3 and 10 indicates a notable increase in temperature with increasing the electrical current (from 125 °C to 250 °C).

In Fig. 12, the surface of metal and plastic showed that by increasing the laser average power, the laser beam penetration in the metal and even in the polymer has significantly increased and caused the formation of deep cavities on the surface of the plastic and metal interface. The images of the metal represent the melting of metal and plastic

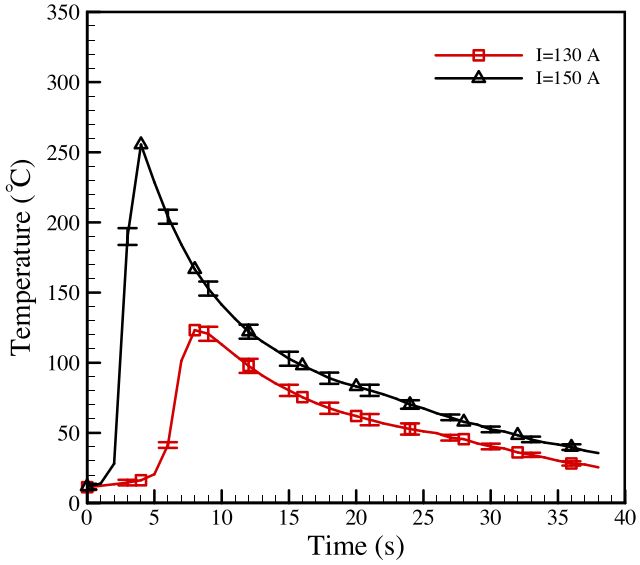

Fig. 11. Experimental results of temperature distribution as a function of electrical current.

particles in the welding zone. Also, amount of melted ABS exited through the steel molten pool surface remarkably increased because of high pulse energy level.

As shown in Fig. 13, in high laser power density, bigger cavities have been formed between metal and plastic. According to the Fig. 13, the white color of sample in Fig. 13. implies that the interface temprature was the highest among these samples.

Comparison the surface of the ABS at the interface of the joint cleary depicts different influences of various pulsed laser process parameters. As shown in Fig.14, the quantity and dimensions of bubbles at the ABS interface joint surface clearly changed. According to the Fig. 14.b, by increasing the pulse frequency from 10 to 15 Hz, the number of bubbles and the width of heat affected zone in the ABS surface remarkably increased comparing to Fig. 14.a. As it is observed in Fig. 14.c, the dimensions, number and also depth of bubbles have evidently incresed compared with Fig. 14.a. Agmentation of the laser current from 130 to 150A has risen depth of heat penetration due to higher level of pulse energy and thereby laser average power.

3.2. Material characterization of polymer-metal surface interface connection zone using the x-ray spectroscopy method

X-ray spectroscopy has been used to analyze the presence of various elements on the surface of the metal (stainless steel 304). With regard to the peaks in the X-ray spectrum in different regions, the presence of different elements was evaluated. The purpose of this analysis is to investigate the presence of ABS particles on the surface of stainless steel. As shown in Fig. 15, X-ray tests was performed in three regions by electron microscope in three regions A, B and C marked fusion area, HAZ and base metal, respectively.

According to the Fig. 16, the largest peak is related to the carbon element. according to the chemical percentage of the elements shown in Table 6, it can be claimed that the lower surface of the molten pool (which is in contact with the ABS part) has the highest carbon content (up to 80% by weight) while the elemental analysis of the base metal showed that it has only about 4% by weight of carbon (Table 7).

Also, it can be noted that hydrocarbon chains of ABS workpiece were located on the bottom of the molten area and were joined and combined to the metal surface. Therefore, it could be concluded that there are some amounts of ABS material on the bottom of fusion zone on the surface of the metal and ABS interconnection. Based on the results, it can be said that there is a definite connection between metal and plastic in this area. In area B (heat affected zone), which is located at a certain distance from the center of the molten pool, the amount of carbon in the graph has dropped to about 24% by weight (see Fig. 17 and Table 8). ABS is a thermoplastic polymer made by polymerizing styrene and acrylonitrile in the presence of polybutadiene. The proportions of the monomer can vary from 15 to 35% acrylonitrile, 5 to 30% butadiene (petroleum hydrocarbon obtained from butane) and 40 to 60% styrene. The polybutadiene component of ABS is the weakest part of ABS that could be easily degraded according to the heat treatment [24].

Hence, the values of ABS elements in this region are lower than the center of the molten pool because by getting away from the center of the melt pool, the values of heat and temperature gradient were reduced and the melted polymer part was decreased. Thus, the joint in this area is weaker than the center of the melt pool. Other elements in the X-ray diffraction spectrum, including iron and chromium are the elements in the stainless steel structure. It can be found that the elements of ABS and stainless steel were combined in the molten pool area and the connection between ABS and stainless steel was established.

3.3. Microstructure analysis of the molten pool

The results of the microstructure study of the welded samples showed the clear microstructure changes in the laser welding zone (molten pool). The images obtained from the optical microscope produced from the etched samples showed the austenite microstructure of the two-strand and delta ferrite strata which commonly observed in

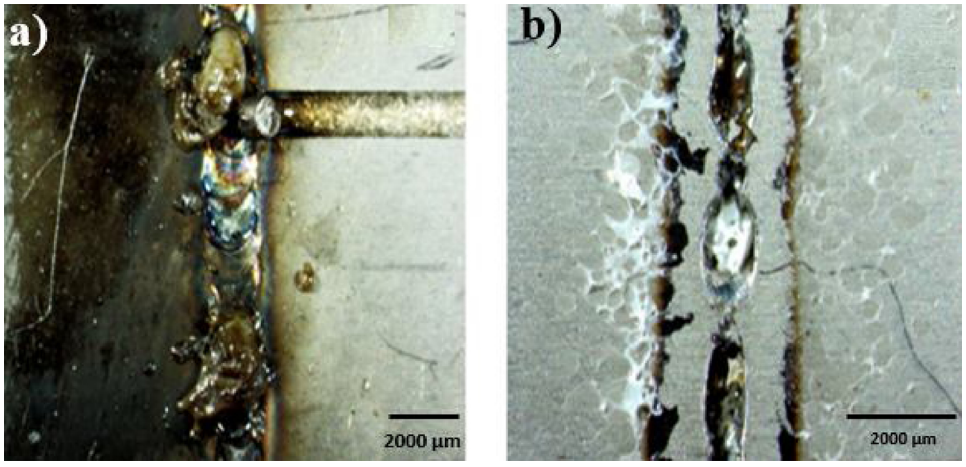

Fig. 12. a) Image of the upper surface of metal and weld bead, b) Image of the lower surface of the polymer.

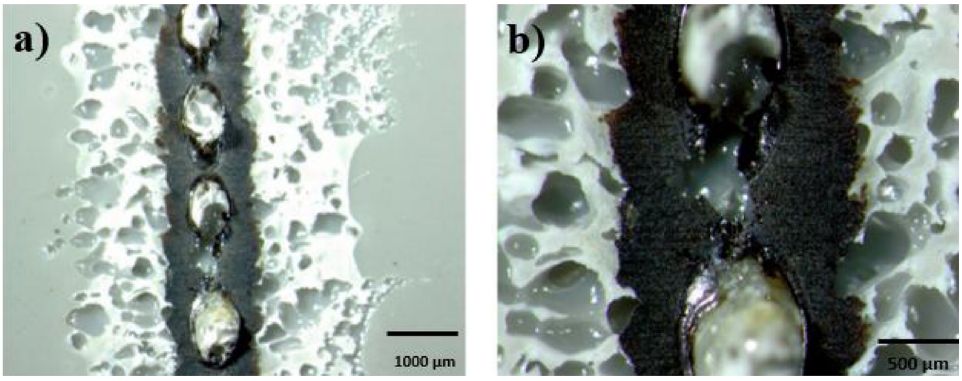

Fig. 13. Cavities and porosities on the surface of the polymer in two magnifications a)20x, b)100×.

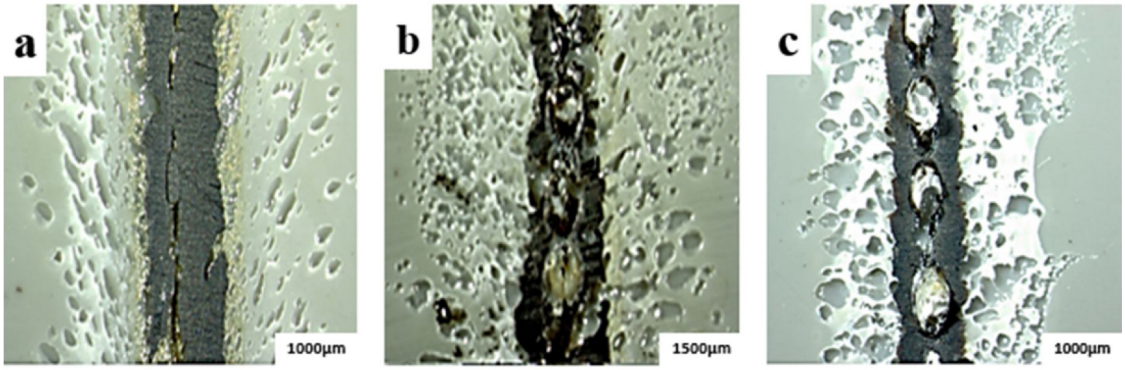

Fig. 14. The ABS interface surface for a) test No.2, b) test No.5, c) test No.11.

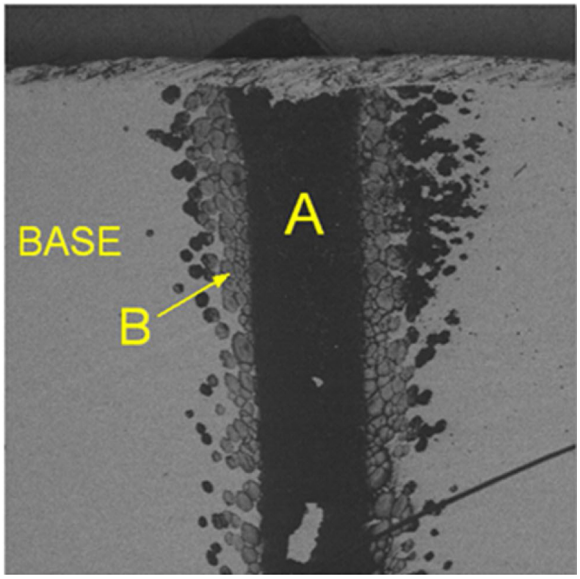

Fig. 15. A) Central region of the molten pool, B) heat affected zone (HAZ) and C) the base metal region away from the welding zone and the molten pool.

austenite stainless steel samples (Fig. 18).

In the area of the molten pool, due to the increase of temperature and reaching the melting point and rapid cooling, the dendritic-austenite microstructure with particles of carbide and amounts of delta ferrite can be observed. Fig. 19 showed the formation of a dendritic microstructure in the molten pool due to the rapid heating, and melting the stainless steel and then the high cooling rate of the molten pool.

Table 9 shows the relation between the laser power and the geometry (depth and width) of the melt pool for stainless steel. Increasing the laser power not only extended the melt pool width but also increased depth of melt pool more significant than width of the melt pool. Therefor, the more weld penetration has produced the higher interface temperature.

3.4. Effect of laser beam power on the shear force

The tensile shear load of the stainless steel-ABS joints was investigated at different levels of the laser powers. As shown in Fig. 20, when the laser power increased from 185 to 215 W, the width of bobble formation area of melted ABS remarkably increased because of increasing the joint interface temperature. Also, the behavior of tensile shear load is observed in Fig. 20. It clearly increased from 280 to 460 N when the laser power incrased from185 to 215. Further increase of the laser power up to 256 W led to reduction of tensile shear load about 15% (395 N).

Seemingly, the laser power has had a significant influence on the shear load and mechanical properties of the joint. According to the Fig. 13, the area of the steel adhered to the ABS surface clearly dimished due to formation of more cavitation and bigger porosities at the joint interface and escaping the molten ABS from the fusion zone of the stainless steel due to excessive heating. Therefore, reduction of the adhesive area of the steel-ABS interface decreased the tensile shear load.

According to the experimental results, the test No. 2 (pulse frequency 15 Hz, pulase duration 8 ms, welding speed 4.2 mm/s, current 130 A and focal length 2 mm) represented the best results among all. Not only the smaller laser beam dimeter iridiated higher power density, but also created high tempreture gradient and narrow heat affected zone in both stainless steel and ABS simultaneously. Seemingly, lower welding speed level and beam diameter have risen the tempreture and thereby produced good weld bead appearance. Additionally, the

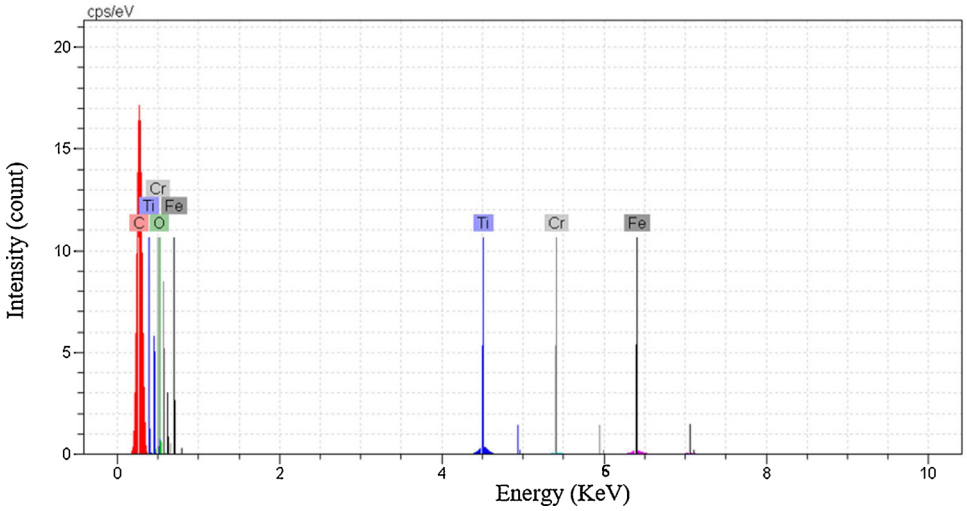

Fig. 16. Result of element analyses by XRD analysis in area A.

Table 6
Weight percentage of the elements in the area of A.

C%	O%	Ti%	Cr%	Fe%	Total%
80.56	15.48	1.59	0.33	2.04	**100**

Table 7
Weight percentage of the elements in base metal.

C%	Si%	Cr%	Mn%	Fe%	Ni%	Total%
4.23	0.41	15.49	1.62	70.32	7.93	**100**

detached surfaces of the joint of test No. 2 reveals the fact that both metal and plastic have existed on either sides of the AISI 304 and ABS joint interface. Clearly, the porosity formation on the ABS surface was observed at lower amounts in comparison to the other tests.

4. Conclusion

- The tensile shear load of the joint increased with laser power from from 280 to 460 N. Increasing the laser power more than 215 W or creating very high interface temperature results in lower shear load

Table 8
Weight percentage of the elements in the area of B.

C%	O%	Si%	Cr%	Mn%	Fe%	Ni%	Total%
24.37	5.24	0.38	12.4	1.43	51.1	5.08	**100**

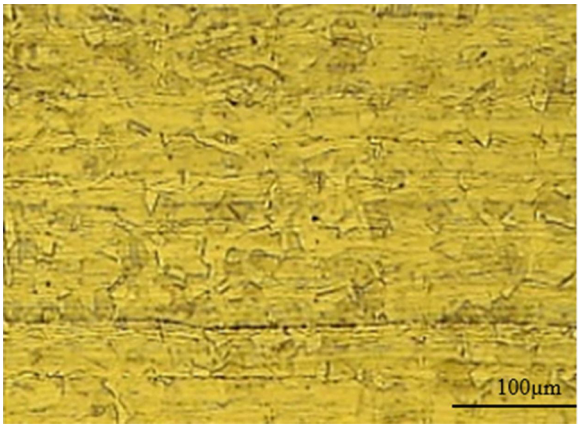

Fig. 18. Base metal microstructure.

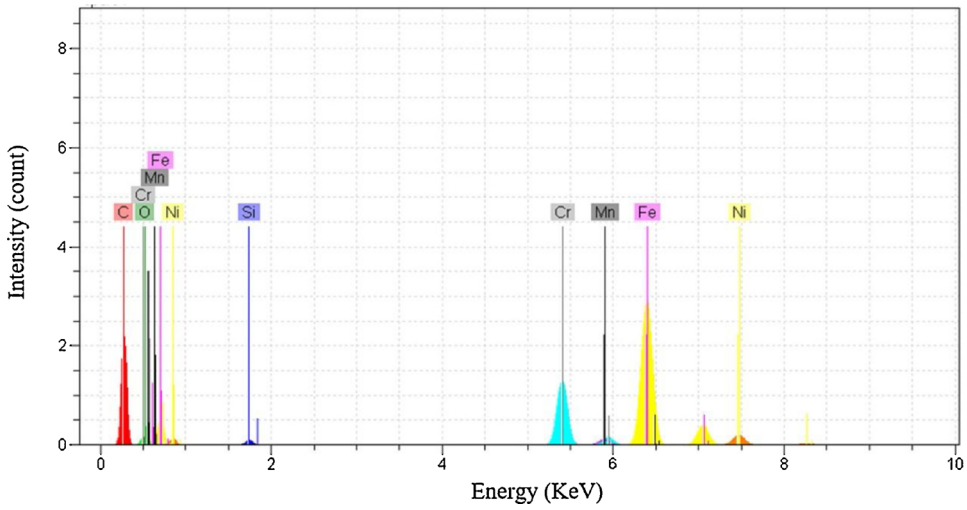

Fig. 17. Result of element analysis by XRD analysis in the area of B.

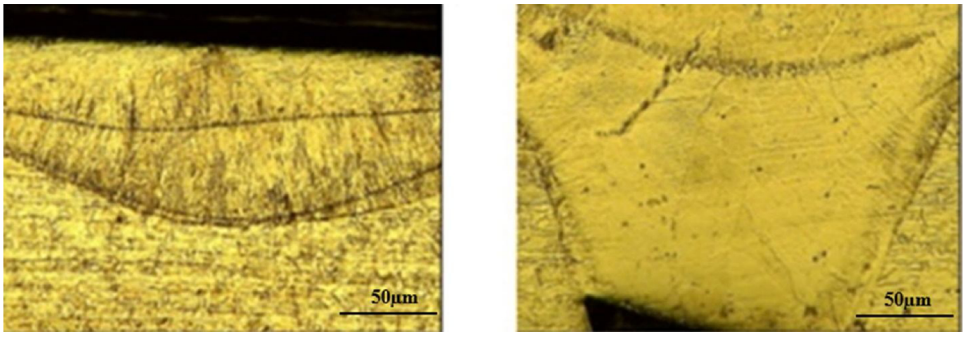

Fig. 19. Microstructure of the AISI 304 fusion zone.

Table 9
Geometry of the stainless steel melt pool at different laser powers.

Test number	Pulse duration (ms)	Frequency (Hz)	Average Power (W)	Welding speed (mm/s)	Melt pool Depth (μm)	Melt pool Width (μm)
3	8	15	215	6.2	75	300
10	8	15	256	6.2	125	350

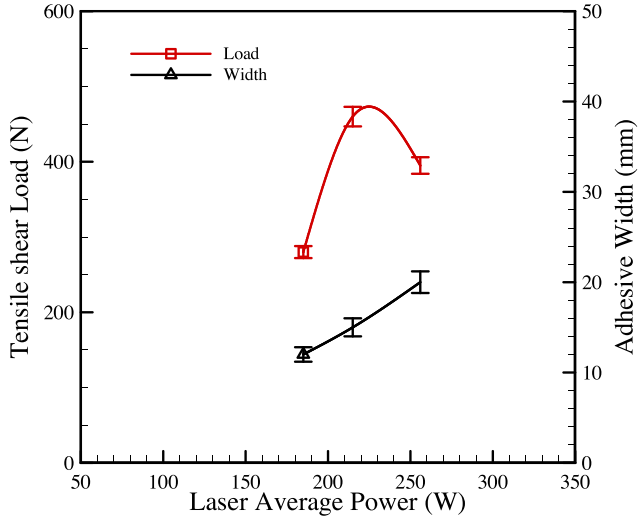

Fig. 20. Tensile shear load variation and adhesive width at different laser beam powers.

due to creating bigger bobbles and more cavities at the adhesive zone.

- By increasing the frequency, the number of bobbled formed at the ABS interface surface was clearly increased. This could be due to higher heating and cooling cycles per unit time.
- Examination of the images of the joint surfaces between the metal and the polymer, revealed the amount of ABS polymer elements at the metal surface which implied that the there is a metal-polymer interface fusion zone.
- According to the results of X-ray analysis, the highest carbon content (up to 80% by weight) at the interconnection zone on the stainless steel surface compared to the base metal carbon content (only about 4%) implys the existance of ABS elements at the fusion zone.
- According to the experiments, it was found that increasing the welding speed, leads to reduction of the temperature because of reducing the interaction time between the laser beam and the amount of molten ABS exited from the steel melt pool decreased due to lower interaction and penetration of laser beam with the ABS.
- By decreasing the laser nozzle gap from the workpiece surface, the laser energy density increased and thereby the surface temperature and the amount of penetration in the metal was significantly increased. Hence, the volume of melted ABS evidently increased and thereby led to formation of plasma pulme, cavitation, spattering and the high amount of melted ABS at the steel melt pool.
- Laser power has a significant influence on the laser beam penetration depth. Hence high power and high energy density leads to the formation of deeper and bigger cavities between metal and plastic. Also the volume of melted ABS clearly increased at higher levels of laser power.

Intellectual property

We confirm that we have given due consideration to the protection of intellectual property associated with this work and that there are no impediments to publication, including the timing of publication, with respect to intellectual property. In so doing we confirm that we have followed the regulations of our institutions concerning intellectual property.

Research ethics

We further confirm that any aspect of the work covered in this manuscript that has involved human patients has been conducted with the ethical approval of all relevant bodies and that such approvals are acknowledged within the manuscript.

Authorship

All listed authors meet the ICMJE criteria. We attest that all authors contributed significantly to the creation of this manuscript, each having fulfilled criteria as established by the ICMJE.

We confirm that the manuscript has been read and approved by all named authors.

We confirm that the order of authors listed in the manuscript has been approved by all named authors.

Contact with the editorial office

This author submitted this manuscript using his/her account in EVISE.

We understand that this Corresponding Author is the sole contact for the Editorial process (including EVISE and direct communications with the office). He/she is responsible for communicating with the other authors about progress, submissions of revisions and final approval of proofs.

We confirm that the email address shown below is accessible by the Corresponding Author, is the address to which Corresponding Author's EVISE account is linked, and has been configured to accept email from the editorial office of American Journal of Ophthalmology Case Reports:

Funding

No funding was received for this work.

Declaration of Competing Interest

No conflict of interest exists.

Acknowledgments

This research is partially supported by the Natural Science Foundation of Guangdong Province, China, (2018A030310522), Shenzhen Science and Technology Planning Project, China, (JCYJ20170818100522101) and Natural Science Foundation of Shenzhen University (2017032).

References

[1] Dimatteo V, Ascari A, Fortunato A. Continuous laser welding with spatial beam oscillation of dissimilar thin sheet materials (Al-Cu and Cu-Al): process optimization and characterization. J Manuf Process 2019;44:158–65.
[2] Yuan R, Deng S, Cui H, Chen Y, Lu F. Interface characterization and mechanical properties of dual beam laser welding-brazing Al/steel dissimilar metals. J Manuf Process 2019;40:37–45.
[3] Chandrasekar G, Kailasanathan C, Vasundara M. Investigation on un-peened and laser shock peened dissimilar weldments of Inconel 600 and AISI 316L fabricated using activated-TIG welding technique. J Manuf Process 2018;35:466–78.
[4] Casalino G, Angelastro A, Perulli P, Casavola C, Moramarco V. Study on the fiber laser/TIG weldability of AISI 304 and AISI 410 dissimilar weld. J Manuf Process 2019;35:216–25.
[5] Jung KW, Kawahito Y, Takahashi M, Katayama S. Laser direct joining of carbon fiber reinforced plastic to zinc-coated steel. Matererials and Design. 2013;47:179–88.
[6] Cheon J, Na S. Relation of joint strength and polymer molecular structure in laser assisted metal and polymer joining. Science Technology Weld Join. 2014;19:631–7.
[7] Zhang Z, Shan J, Tan X, Zhang J. Effect of anodizing pretreatment on laser joining CFRP to aluminum alloy A6061. Int J Adhes Adhes 2016;70:142–51.
[8] Camanho P, Fink A, Obst A, Pimenta S. Hybrid titanium-CFRP laminates for high-performance bolted joints. Compos Part A Appl Sci Manuf 2009;40:1826–37.
[9] Kelly G. Quasi-static strength and fatigue life of hybrid (bonded/bolted) composite single-lap joints. Compos Struct 2006;72:119–29.
[10] Ai Y, Zheng K, Shin Y, Wu B. Analysis of weld geometry and liquid flow in laser transmission welding between polyethylene terephthalate (PET) and Ti6Al4V based on numerical simulation. Opt Laser Technol 2018;103:99–108.
[11] Wang X, Li P, Xu Z, Song X, Liu H. Laser transmission joint between PET and titanium for biomedical application. J Mater Process Technol 2010;210:1767–71.
[12] Noha FS, Zina HM, Alnasser Kh, Yusoff N, Yusof F. Optimization of Laser Lap Joining between Stainless Steel 304 and Acrylonitrile Butadiene Styrene (ABS). Procedia Eng 2017;184:246–50.
[13] Cenigaonaindia A, Liebana F, Lamikiz A, Echegoyen Z. Novel strategies for laser joining of polyamide and AISI 304. Phys Procedia 2012;39:92–9.
[14] Pelsmaeker JD, Graulus GJ, Vlierberghe SV, Thienpont H, Hemelrijck DV, Dubruel P, et al. Clear to clear laser welding for joining thermoplastic polymers: A comparative study based on physicochemical characterization. J Mater Process Technol 2018;255:808–15.
[15] Xianghu T, Jing Z, Jiguo S, Yang S, Jialie R. The damage characteristics and mechanism of CFRP during laser joining of CFRP/mild steel dissimilar joint. ICALEO 2013;2013:582.
[16] Zhan Z, Tan XH, Zhang J, Shan JG. Suppression of shrinkage porosity in laser-joining of CFRP and steel using a laser surface modification process "Surfi-Sculpt". Int J Adhes Adhes 2018;85:184–92.
[17] Katayama S, Kawahito Y. Laser direct joining of metal and plastic. Scr Mater 2008;59:1247–50.
[18] Hussein FI, Akman E, GencOztoprak B, Gunes M, Gundogdu O, Kacar E, et al. Evaluation of PMMA joining to stainless steel 304 using pulsed Nd:YAG laser. Opt Laser Technol 2013;49:143–52.
[19] Bhattacharya R, Kumar N, Kumar N, Bandyopadhyay A. A study on the effect of process parameters on weld width and heat affected zone of pulsed laser welding of dissimilar transparent thermoplastics without filler materials in lap joint configuration. Mater Today Proc 2018;4:3674–81.
[20] Lambiase F, Genna S. A procedure for calibration and validation of FE modelling of laser-assisted metal to polymer direct joining. Opt Laser Technol 2018;68:363–72.
[21] Lambiase F, Genna S. Experimental analysis of laser assisted joining of Al-Mg aluminium alloy with Polyetheretherketone (PEEK). Int J Adhes Adhes 2018;84:265–74.
[22] Gisario Annamaria, Mehrpouya Mehrshad. Dissimilar joining of transparent Poly (ethylene terephthalate) to aluminum 7075 sheets using a diode laser. J Laser Appl 2018;29:022418.
[23] Chen Z, Huang Y, Hana F, Tang D. Numerical and experimental investigation on laser transmission welding of fiberglass-doped PP and ABS. J Manuf Process 2018;31:1–8.
[24] McKeen Laurence W. The effect of long term thermal exposure on plastics and elastomers. Elsevier Inc; 2014.